

NON-DESTRUCTIVE DIAGNOSTICS OF BRIDGE STRUCTURES

by

Alexandru Cotofan, Dipl. Eng., (*Gemite Romania SRL*), Ivan Razl, Ph.D., P.Eng (*Gemite Products Inc*)
and Spiridon Cretu, Prof. Dr. Ph.D., P.Eng. (*Technical University Gh. Asachi from Iasi, Romania*)

Abstract: *V současné době existuje řada non-destruktivních metod, které se mohou použít k diagnostice železničních nebo silničních železobetonových mostů. Metody nám umožňují získání přesných informací o elektrickém odporu betonu, pravděpodobnost a míru koroze, skryté defekty, uložení armovacího železa a rigidity konstrukce. Diagnostické metody též stanoví koncentraci chloridových iontů a hloubku karbonátace. Článek též uvádí výsledky diagnostiky dvanácti mostů v západním Rumunsku.*

In the following article non-destructive diagnosis techniques are presented, together with the equipment used, interpretation methods and results from field investigations. The procedures briefly presented, which have been used to diagnose 12 bridges, include: the radar scanning with 3D imaging, the pull out test, the impact-echo technique, pH of concrete measurements, permeability and corrosion rate measurements.

The Radar scanning and 3D visualizations.

The Radar (*acronym from Radio Detection and Ranging*) technique use electromagnetic pulses with frequencies over 1 GHz, which penetrate concrete up to 1 m and produce high resolution images from the reflected waves by the embedded volumes of different dielectric characteristics. The reflection coefficient of the waves, according to the **Expression 1**, is related to the relative dielectric constant ϵ_{r1} of the material through which the incident waves arrives, and ϵ_{r2} for the discontinuity that produces the reflection.

$$(1) \quad \rho_{1,2} = \frac{\sqrt{\epsilon_{r1}} - \sqrt{\epsilon_{r2}}}{\sqrt{\epsilon_{r1}} + \sqrt{\epsilon_{r2}}}$$

The values of relative dielectric constants vary from 1 for air, to 6-12 for concrete, and over 80 for water. The best 3D reflected images are obtained for steel and cracks/faults damped/filled with water. The embedded dry voids are difficult to be visualized as the reflection coefficient is below 50%.

The equipment used was a CONQUEST system, with frequencies over 1 GHz, that may also analyze the magnetic signature of rebar. The data have been processed in “slices” with CONQUEST-VIEW or 3D with VOXLER.

For the 12 bridges, the Radar scans were used over reinforced concrete columns and beams, mainly for two reasons:

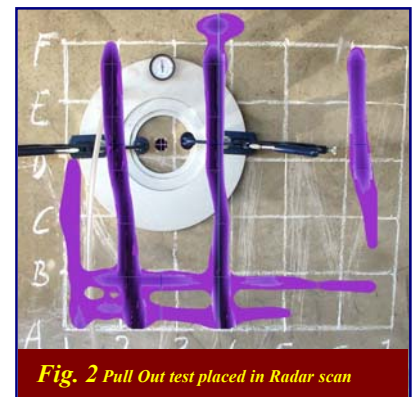
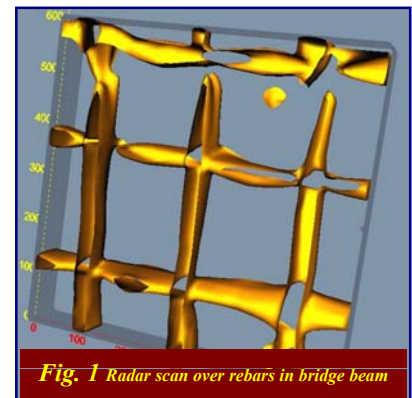
A. To examine the placement of the reinforcing steel (see **Fig. 1**) in the existing structures. We applied this technique in conjunction with a reluctance covermeter, to verify by the second method the depth and the rebar diameter, obtained by the Radar scanning. The results from Radar scanning and magnetic investigations were used as input data in:

- i. the polarization technique, to determine the probability and the rate of rebar corrosion;
- ii. Mathematical evaluation of the structure rigidity, together with additional data obtained by methods described below.

B. To precisely locate the rebar, information that allows an accurate placement of the pull out test for concrete strength measurement, (see **Fig. 2**) with a super-imposed radar image over the test area.

The Radar scanning is the first step in the nondestructive diagnosis for each bridge, preparing the base set of information for the subsequent techniques:

- Locating the rebar position;
- Reinforcement cover;
- Providing together with covermeter the rebar diameter;
- Visualizing the degree of corrosion;
- Locating the ducts with the post-tensioned tendons.



The Pull Out tests.

The technique consists in coring an 18.4 mm hole, perpendicular to a planed surface, outside of the reinforcement disturbance. A recess is routed in the hole to a diameter of 25 mm and depth of 25 mm. A split ring is expanded in the recess and pulled against a counter pressure, 55 mm inner diameter, placed on the surface concentrically with the ring. The concrete in the strut between the expanded ring and the counter pressure is being compressed; hence the pull-out force “*F*” is related to compressive strength of the concrete (see **Fig. 3**).

The test is partially destructive, as it has to be performed until the cone between the expanded ring and the inner diameter of the counter pressure is dislodged (**Fig. 4**).

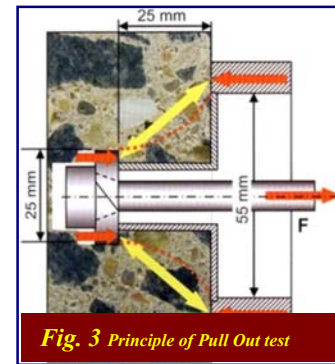


Fig. 3 Principle of Pull Out test



Fig. 4 Broken cone after Pull Out test

The relations used in the conversion of the pull-out force *F* are provided by the set of **Expressions 2**.

$$\begin{aligned} f_{cube} &= 0,76 \cdot F^{1,16} \\ f_{cyl} &= 0,69 \cdot F^{1,12} \end{aligned} \quad (2)$$

Where f_{cube} and f_{cyl} are the compressive strengths related to those of cubes and cylinders. With a 95% confidence level, and for an average of 4 tests, the compressive strength measurement precision is within $\pm 6\%$ compared to standard specimen tests (cylinders, cubes or cores) for a maximum aggregate size of 38 mm. On normal concrete the variation of the test is in the range of $\pm 8\%$. Most importantly, the technique is not affected by stresses developed in the structure.

The equipment used is a GERMANN system, with a hydraulic pull-out machine, that logs the peak values of the force “*F*”. The apparatus is designed, produced and calibrated under ASTM C 900-99 and BS 1881 part 207.

On each bridge we have quantified the strength of the concrete from columns and beams by using the pull-out test. The coring positions outside of the reinforcement disturbance are established by Radar scan (**Fig. 2**).

Table 1

The test results are presented in the **Table 1**. Each pull-out value from the table is an average of three tests. σF_{cube} is the compressive strength of the tested concrete, computed from the pull out force “*F*” using **Expressions (2)**. On two bridges the pull-out tests were conducted over all structural elements for a complete assessment of columns and beams. The special need for these two bridges, (41 Km + 579 m) and (86 Km + 236 m) arrived from our tests results through impact-echo method, through which we checked the injection of the ducts of the post tension tendons. For all bridges, the results from the pull-out method were verified using the impact-echo technique, by measuring the wave speed at the concrete surface, and computing the Young modulus and compressive strength.

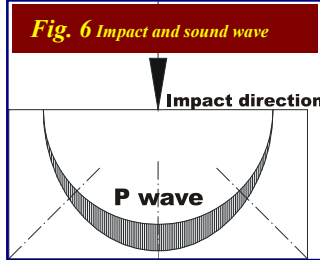
The Impact-Echo technique.

Since the impact-echo method is relatively new, when compared with the rest of the methods used, we shall describe this method in more detail. The impact-echo method, introduced by Carino and N.J. Sansalone in 1986, has become a powerful tool in finding any variation of sonic impedance in the concrete. The method is very similar to the radar technology. But, the impact-echo is sensitive to dry voids only, cracks and steel presence, versus the radar system, which is very sensitive to moisture, water and steel, as it exploits the variations in magnetic permittivity. Due to the accuracy of the results, the impact-echo technique was chosen to be the standard technology for quality control of tunnels in Germany. It seems that impact-echo is the first non-destructive technology to be part of regulating standard for Quality Control in civil engineering in Germany and other parts of Europe. The method is suitable for a wide class of tests, allowing determination of concrete compressive strength and Elastic Modulus by evaluating the sound speed. It measures the thickness of the structure, locates voids, delaminations, honeycombing and layers of different materials (e.g. incorporated

DN 79 Arad - Timisoara	Beam or deck	Column
[Km + m]	σF_{cube} [MPa]	σF_{cube} [MPa]
10 + 324 old section	26,6	
10 + 324 new section		
33 + 189	61,9	
38 + 628	14,5	
41 + 579	56,1	34,8
46 + 100	42,8	
48 + 000		38,5
53 + 183		72,9
86 + 236	28,8	32,8
87 + 100	41,1	
88 + 940	61,6	
91 + 250	92,3	
95 + 250	52,5	

waterproofing membranes), establish the areas of corrosion as well as the corrosion degree of steel reinforcement and may measure the depth of cracks.

The method uses transient stress waves generated on the surface of concrete or masonry structures through a small, elastic energy impact. The energy is transmitted to concrete through an impact with a small steel ball (**Fig. 5**), whose diameter in general may vary between 1 to 24 mm, which define the wave length and consequently the fault dimensions that may be found.



The main impulse is traveling through the concrete as a compressive wave, having a hemispheric front (**Fig. 6**).

According to the **Expression (3)**, the wave speed is related to following concrete parameters:

- “**E**” (the Young modulus),
- “**ρ**” (the specific gravity) and
- “**ν**” (the Poisson coefficient).

$$C_P = \sqrt{\frac{E}{\rho} \cdot \frac{(1 - \nu)}{(1 + \nu)(1 - 2\nu)}} \quad (3)$$

As the stress waves propagate through the material being tested, these are reflected by the internal interfaces (discontinuities in the material with different acoustic impedances, such as delaminating layers, voids, honeycombing and cracks, as well as steel elements) and by the external boundaries of the structure. The way to compute the distance “**h**” between the impact point and the discontinuity using a frequency “**f**” from the echo spectrum and the pre-measured sound speed “**C_P**”, depends on the value of the acoustic impedance of the discontinuity:

- For lower acoustic impedances than concrete (as cracks, voids) the **Expression 4** is used. $h = \frac{C_P}{2 \cdot f} \quad (4)$
- For higher acoustic impedances than concrete (as steel elements) the **Expression 5** is used. $h = \frac{C_P}{4 \cdot f} \quad (5)$

All bridge elements tested through the pull-out method were re-tested with the impact-echo technique to determine the sound speed “**C_P**” (**Fig. 7**). The equipment is manufactured by GERMANN Instruments in conformance with ACI 228.2 R.



The specific gravity used in the **Expression 3** is an average measured over all cores extracted during the pull-out preparation tests.

The average values are:

- 2,4 g/cm³ for the specific gravity, and
- 0,20 for the Poisson Ratio coefficient.

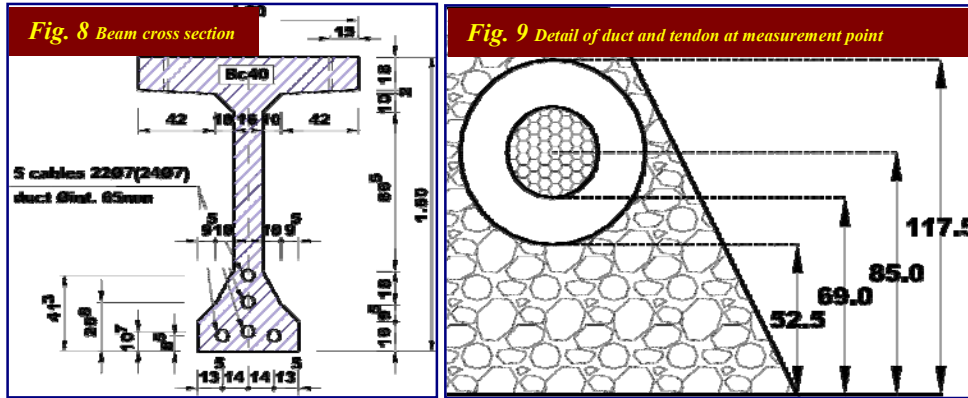
All findings are listed in **Table 2**. The “**σ_{F_{cube}}**” is the compressive strength work out from the pull-out force “**F**” through **Expressions 2**, for which the concrete “**Class_{from σ_{F_{cube}}}**” is assumed. “**C_P**” is the sound speed measured by Impact-Echo and “**E**” is the Young modulus computed with **Expression 3**, for which the concrete “**Class_{from E}**” is again deduced.

The concrete strengths obtained through impact-echo are similar to those obtained through pull-out method.

Table 2

DN 79 Arad - Timisoara		Beam or deck				Column				
Km+m	σF_{cube} [MPa]	Class from σF_{cube}	C_p [m/sec]	E [N/mm ²]	Class from E	σF_{cube} [MPa]	Class from σF_{cube}	C_p [m/sec]	E [N/mm ²]	Class from E
10 + 324 old section	26,6	Bc 25						3.514	28.941	Bc 25
10 + 324 new section			4.299	43.315	Bc 50					
33 + 189	61,9	Bc 60	4.234	42.015	> Bc 50			4.115	39.687	Bc 50
38 + 628	14,5	Bc 10	3.031	21.531	Bc 10					
41 + 579	56,1	Bc 50	3.946	36.494	> Bc 40	34,8	Bc 30			
46 + 100	42,8	Bc 40	4.113	39.648	Bc 40					
48 + 000						38,5	Bc 35	4.299	43.315	Bc 40
53 + 183			5.052	59.818	> Bc 60	72,9	Bc 60			
86 + 236	28,8	Bc 25				32,8	Bc 30			
87 + 100	41,1	Bc 40						3.891	35.484	Bc 35
88 + 940	61,6	Bc 60						4.361	44.574	Bc 50
91 + 250	92,3	Bc 60								
95 + 250	52,5	Bc 50						3.388	26.902	Bc 20

By using the impact – echo, we have also examined the grouting of the ducts for post-tensioned tendons on bridge (Km 41 + 579 m). The bridge has three spans, each 40 m long. The impact-echo tests were done over the central span, on one of the exterior concrete beams. The beam cross section at the test point is shown in **Fig. 8**. The geometrical details for the tested duct and tendon are shown in **Fig. 9**.



The thin steel layers under 3 mm thickness, do not interfere with the impact-echo method. Due to this characteristic, the steel duct is totally transparent to the sound waves and the quality of the grout injection can be measured. During the tests three situations may be found, depending on the injection quality:

- Duct fully grouted, when the grout fills completely the volume from 52,5 mm to 117,5 mm;
- Duct with air pocket, when the grout fill the volume from 52,5 mm to any level between 69,0 and 117,5 mm;
- Duct un-grouted, with an ineffective grout injection between 52,5 to 69,0 mm.

The sound speed in the concrete beam bridge from Km 41 + 579 m is 3.946 m/sec (see **Table 2**). The three different situations described above generate three different echo spectra:

- The duct fully grouted return only one echo frequency corresponding to the tendon placed at 85 mm. The frequency is computed with the **Expression 5**, from which is resulting the **Expression 6**.

$$(6) f_T = \frac{3.946 \left[\frac{m}{sec} \right]}{4 \cdot 85 [mm]} = 11,6 [KHz] \quad tendon$$

- The duct partially grouted will return a frequency corresponding to the tendon, but also one corresponding to the position of the air surface in the duct, computed with the **Expression 4**, and is resulting the **Expressions 7**.

$$(7) f_{PGM} = \frac{3.946 \left[\frac{m}{sec} \right]}{2 \cdot 69 [mm]} = 28,6 [KHz] \quad grout \ level: \ 85 \ mm \quad f_{PGm} = \frac{3.946 \left[\frac{m}{sec} \right]}{2 \cdot 117,5 [mm]} = 16,8 [KHz] \quad grout \ level: \ 117,5 \ mm$$

- The un-grouted duct will return only the echo of the air surface that may be placed between 52,5 to 69 mm, and which is also computed with the **Expression 4**, from which is resulting the **Expressions 8**.

$$(8) f_{UGM} = \frac{3.946 \left[\frac{m}{sec} \right]}{2 \cdot 52,5 [mm]} = 37,6 [KHz] \quad grout \ level: \ 52,5 \ mm \quad f_{UGm} = \frac{3.946 \left[\frac{m}{sec} \right]}{2 \cdot 69 [mm]} = 28,6 [KHz] \quad grout \ level: \ 85 \ mm$$

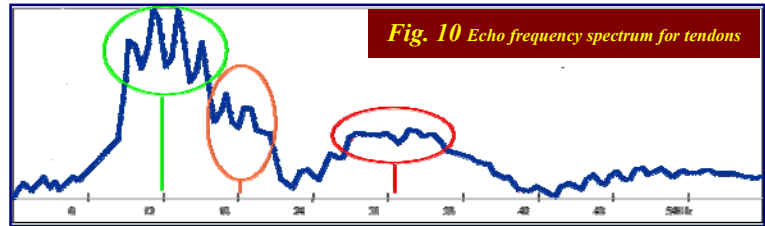
The site tests may be done only after pre-computing the expected frequencies. To the logged echo in the site, we applied a Fast Fourier Transformation and we obtained the spectrum of frequencies. The spectrum diagram is presented in **Fig. 10**. All pre-computed frequencies appear in the spectrum diagram, indicating:

At the measurement point the ducts are partially injected, as computed under the above (ii) situation:

- The develop to the f_T frequency at 11,6 KHz (in the green balloon) indicate that the tendon is embedded in the grout;
- The emerge of a frequency band scattered around 18 KHz (in the orange balloon) shows that the voids in the duct are located between 69,0 mm and 117,5 mm;

But also, in neighborhoods exists un-injected areas, as computed under the above (iii) situation:

- A frequency band scattered around 31 KHz (in the red balloon) shows that close to the tested point the duct is not injected; the grout in the duct is located between 52,5 mm and 69,0 mm;



For a complete assessment of bridges we carried out supplementary tests for concrete permeability and acidity.

The Permeability tests.

The permeability was tested with the CLAM equipment produced by GERMANN Instruments, manufactured in conformance with EN-ISO 7031 (**Fig. 11**). The concrete permeability is estimated through the permeability coefficient, in accordance with **Expression 9**.

$$C_{cp} = \frac{B \cdot (g_1 - g_2)}{A \cdot t} \cdot \frac{L}{P} \quad (9) \quad , \text{ in which}$$

B , L and A are the equipment constants;
 g_1 and g_2 micrometer indications;
 P is the working pressure, and
 t the measured time.



The tests were done at 1 bar pressure. The pressure is kept constant, to compensate the water infiltrations in concrete, by adjusting the micrometer plunger. The volume of water “pushed” into the concrete is the equivalent of 25 microns plunger movement. The time needed by the water volume to penetrate, defines finally the permeability. The results are given in **Table 3**. C_{PB} is the permeability coefficient computed with the **Expression 9**.

pH Measurements.

These tests were carried out on the 18,4 mm diameter cores, obtained during the preparation process for the pull out tests. The cores were tested using pH indicators and the pH values (**Fig. 12**) are given in **Table 4**.

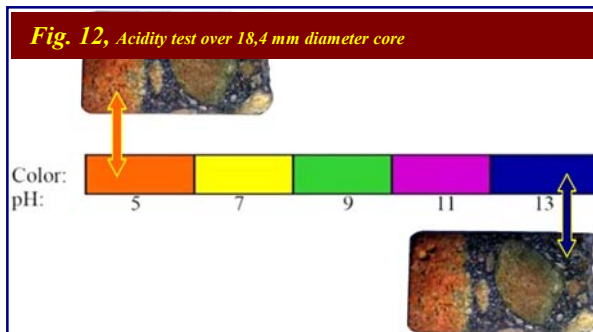


Table 3

[Km + m]	C_{PB} [mm ² /s·Bar]
10 + 324 old section	1,06 x 10 ⁻¹
10 + 324 new section	
33 + 189	1,92 x 10 ⁻⁴
38 + 628	4,88 x 10 ⁻¹
41 + 579	3,32 x 10 ⁻³
46 + 100	9,75 x 10 ⁻²
48 + 000	8,85 x 10 ⁻²
53 + 183	1,95 x 10 ⁻¹
86 + 236	4,64 x 10 ⁻¹
87 + 100	2,10 x 10 ⁻¹
88 + 940	1,50 x 10 ⁻¹
91 + 250	1,01 x 10 ⁻⁴
95 + 250	3,11 x 10 ⁻¹

Table 4

A good correlation exists between the concrete permeability and pH (**Table 5**). The higher permeability corresponds to lower pH.

Table 5

DN 79 Arad - Timisoara [Km + m]	pH structure	C _{PB} [mm ² /s·Bar]
10 + 324 old section	7	1,06 x 10 ⁻¹
38 + 628	5	4,88 x 10 ⁻¹
53 + 183	5	1,95 x 10 ⁻¹
86 + 236	5	4,64 x 10 ⁻¹
87 + 100	5 / 13	2,10 x 10 ⁻¹
88 + 940	5 / 11	1,50 x 10 ⁻¹
95 + 250	5	3,11 x 10 ⁻¹

DN 79 Arad - Timisoara [Km + m]	Beam or deck pH	Pile pH
10 + 324 old section	7	
10 + 324 new section		
33 + 189	11	
38 + 628	5	
41 + 579	13	
46 + 100	13	
48 + 000		11
53 + 183		5
86 + 236	5	5
87 + 100	5 / 13	
88 + 940	5 / 11	
91 + 250	13	
95 + 250	5	

Polarization Method.

The corrosion rate of steel rebar was measured using the polarization method, with the rebar acting as a working electrode. Galva-Pulse equipment manufactured in conformance with ASTM C 876, and using an Ag/Ag-Cl electrode was used for the site tests (**Fig. 13**). The equipment polarizes the steel rebar under a certain established drop of potential, and computes the corrosion loss of mass, using the Faraday law, according to **Expression 10**.

$$X_{corr} = 302 \cdot \frac{I_P}{A \cdot \Delta E_P} \quad (10)$$

in which:

- X_{corr}** is the loss of mass through corrosion
- A** is the polarized area from the rebar
- I_P** is the polarization current
- ΔE_P** is the potential drop between the working and counting electrode.

The rate of corrosion was measured at four bridges.

The results are presented graphically as echi-potential maps, containing the rate (**Fig. 14**) and the corrosion probability.

The maximum loss of mass for the four tested bridges, are listed in the **Table 6**. **V_{cor}** is the steel loss from the reinforcing, given in [μm/year] on the rebar radius and it is provided directly by Galva-Pulse, by computing the **Expression 10**.

DN 79 Arad - Timisoara [Km + m]	pH structure	V _{cor} [μm/year]
10 + 324 old section	7	1,06 x 10 ⁻¹
38 + 628	5	4,88 x 10 ⁻¹
41 + 579	13	1,95 x 10 ⁻¹
53 + 183	5	4,64 x 10 ⁻¹

Table 6

No serious rebar corrosion was found, even in areas where the pH values of concrete were under pH 5.

Conclusions:

The methods described provide fast and accurate tools for quality-control and diagnosis of infrastructure, industrial and civil structures. The results have high reproducibility, and may be cross-checked through different methods.



Fig. 13 Test of rebar corrosion with Galva Pulse

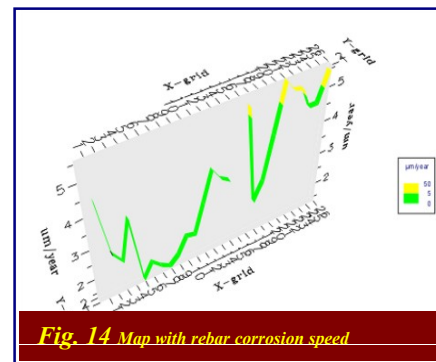


Fig. 14 Map with rebar corrosion speed

Using the techniques described in the article we succeeded to evaluate 12 bridges during a period of 6 working days, in November 2007. Two of them, as result of our findings, are already being repaired. The techniques were also used with success by the authors in evaluation of other structures such as railway bridges, runways of major airports or in waste water treatment facilities. In all diagnostic projects the testing time was short and no destructive methods were needed for conducting the tests.